Chem. Res. Chinese Universities, 2019, 35(1), 47—52 doi: 10.1007/s40242-019-8295-2

Effect of Cesium Modification on CuO/CeO_2 Catalysts for the Catalytic Decomposition of N_2O

GUO Peiwen, QIN Feng, SUN Chao, HUANG Zhen, SHEN Wei and XU Hualong*

Shanghai Key Laboratory of Molecular Catalysis and Innovative Materials, Laboratory of Advanced Materials, Collaborative Innovation Center of Chemistry for Energy Materials, Department of Chemistry, Fudan University, Shanghai 200433, P. R. China

Abstract A series of Cs-modified CuO/CeO_2 mixed oxide catalysts was prepared for enhancing the stable activity of N_2O decomposition. It was found that Cs modification promoted the catalytic performance of CuO/CeO_2 catalysts significantly. The 1%Cs-CuO/CeO_2 catalyst exhibited the best activity, and the conversion of N_2O reached 100% at 380 °C in the presence of 2% O_2. The catalytic behaviors were investigated by means of XRD, N_2 adsorption isotherms, XPS, H_2-TPR(TPR: temperature-programmed reduction), CO-IR, O_2-TPD(TPD: temperature-programmed desorption) and diffused reflectance infrared Fourier transform spectorscopy(DRIFTs). The results revealed that Cs modification promoted the activity and the oxygen resistance by enhancing the desorption of surface oxygen species and increasing the content of Ce^{3+}. CO-DRIFTs revealed that Ce^{3+} could efficiently facilitate the regeneration of active Cu^+ sites by an oxygen migration step. The possible reaction mechanism was also discussed.

Keywords Cs-Modified CuO/CeO_2; N_2O decomposition; Reaction mechanism

1 Introduction

Nitrous oxide(N_2O) is a major greenhouse gas with a long lifetime of approximately 150 years in the atmosphere. The global warming potential(GWP) of N_2O is 310 times higher than CO_2[1,2]. Furthermore, it contributes to stratospheric ozone depletion[3]. The concentration of N_2O in the atmosphere has been increasing recently mainly because of human activities, particularly chemical manufacturing. Thus, it is urgent to develop efficient methods for N_2O removal from industrial exhaust gases. Considering efficiency and cost, direct catalytic N_2O decomposition technology is a superior choice.

Various types of catalysts have been investigated to promote N_2O degradation, such as noble metals[3—5], metal oxides[6—8], and zeolites[9—11]. Among them, Ce-based mixed metal oxides have a great advantage because of low cost and excellent catalytic activity. They have been widely applied for N_2O decomposition in forms, such as CuCe, NiCe and FeCe catalysts[12—18].

In our previous work, CuCe mixed oxide catalysts exhibited high efficiency for N_2O decomposition[13], and we also revealed that Cu^+ is the active site. The desorption of generated oxygen was considered as the rate-determining step for N_2O decomposition: $2Cu^{2+}\text{-}O \longrightarrow 2Cu^{+}+O_2$. Zabilskiy *et al.*[16,17] synthesized various CuO/CeO_2 catalysts with different nano-CeO_2 supports and proposed another pathway, in which Ce^{3+} participated in the regeneration of the active Cu^+ sites: $Cu^{2+}\text{-}O+Ce^{3+} \longrightarrow Cu^{+}+Ce^{4+}\text{-}O$. Konsolakis *et al.*[18] investigated the catalytic decomposition of N_2O over CuO-CeO_2 catalysts prepared by different synthesis routes, and coprecipitation was found to be the best route. However, few of the CuCe mixed oxide catalysts were effective enough for commercial application because their activities were severely inhibited by other gases, such as O_2[15—18]. Therefore, the issue of activity improvement and oxygen resistance should be solved promptly.

Alkali doping was found to be an efficient method to improve the activity of N_2O decomposition over single-metal oxide catalysts(CuO, NiO and Co_3O_4)[18—22]. It was revealed that alkali modification improved the reducibility of the transition metal and enhanced the regeneration of active sites. Additionally, Cs showed the best promotion effect among alkali metals[23]. To the best of our knowledge, there is little research on the effect of alkali modification over CuO/CeO_2 mixed metal oxide catalysts. Furthermore, the reaction pathway of N_2O decomposition over CuO/CeO_2 catalysts is inconsistent[13—18].

In the present work, Cs modification was applied to improve the activity and oxygen resistance of the CuO/CeO_2 catalyst. The effects of Cs promotion and a possible reaction pathway were also discussed.

2 Experimental

2.1 Materials

CuO/CeO_2 was prepared by the citric acid method[13], and

*Corresponding author. Email: shuhl@fudan.edu.cn

Received September 13, 2018; accepted October 15, 2018.

Supported by the National Key R&D Program of China(No.2017YFB0602204), the National Natural Science Foundation of China(No.91645201) and the Shanghai Science and Technology Committee Fund, China(No.14DZ2273900).

a series of Cs-modified CuO/CeO_2 catalysts with Cs of 0, 0.25%, 0.5%, 1.0%, 2.0% and 4.0%(molar fraction) were prepared by the impregnation method[19]. $Cu(NO_3)_2·3H_2O$, $Ce(NO_3)_3·6H_2O$ and citric acid(1:1:4, molar ratio) were dissolved in water under continuous stirring. An amorphous precursor was acquired after the solution was dried at 80 °C overnight, then dried at 120 °C for 6 h. The precursor was calcined at 550 °C for 4 h to acquire the mixed oxide. Cs-modified CuO/CeO_2 catalysts were obtained by impregnation with an aqueous solution of $CsNO_3·H_2O$. The samples were dried at 120 °C, then the catalysts were calcined at 550 °C for 4 h in air. The Cs to (Cu+Ce) molar ratio was varied from 0 to 4.0%, and the catalysts were denoted as *y*%Cs-CuO/CeO_2(*y*=0.25—4).

2.2 Characterization

A Bruker D8 powder X-ray diffractometer was operated at 40 kV and 40 mA to record XRD patterns. The patterns were taken over a 2θ range from 10° to 80° with a step size of 0.02°. The surface areas of the BET model were measured on a Micromeritics TRISTAR 3000 apparatus. XPS results were recorded on a Perkin Elmer PHI5000C system, and the binding energy was calibrated by the carbonaceous C_{1s} line(284.6 eV).

A Micromeritics AutoChem II 2920 equipped with a TCD detector was used to obtain the H_2-TPR(TPR: temperature-programmed reduction) data. A sample of 0.05 g was pretreated in He at 200 °C for 1 h and cooled to 25 °C. Next, the sample was reduced in H_2/Ar(5% H_2, volume fraction) with a heating rate of 10 °C/min. O_2-TPD(TPD: temperature-programmed desorption) was also carried out on the AutoChem II 2920. Samples were pretreated in a helium stream at 400 °C for 1 h, and then an O_2-He mixture(5% O_2, volume fraction) was introduced into the reactor for 1 h after cooling down to 30 °C in helium. Afterwards, the samples were heated to 600 °C in helium to analyze the effluent gases.

The CO-IR and diffused reflectance infrared Fourier transform spectorscopy(DRIFTs) were carried out on an FTIR(Nicolet 6700) spectrometer. For CO-DRIFTs, samples were pretreated under corresponding conditions, then cooled down to 50 °C in He flow. Spectra were collected after the 1% CO-He mixture had been introduced into the system for 30 min. For *in situ* N_2O-DRIFTs, spectra were collected after the samples had reacted with 2600 μL/L N_2O-He mixture at various temperatures for 1 h.

2.3 Activity Tests

An automated 8-flow reactor system was used to evaluate activities for N_2O catalytic decomposition. Approximately 250 mg of catalyst(40—60 mesh) was packed in the middle part of a quartz reactor. The sample was pretreated in helium at 400 °C for 1 h and then cooled down to 260 °C. The activity was tested in a gas mixture(2600 μL/L N_2O in He) with a gas flow of 60 mL/min(GHSV=19000 h^{-1}). The products were analyzed by a Finnigan Trace GC Ultra. The activity tests under an O_2-containing atmosphere were carried out under the same conditions, except for an extra 2% O_2 in the reaction gas.

3 Results and Discussion

3.1 Textural Properties of Cs-Modified CuO/CeO_2 Catalysts

XRD patterns of Cs-modified CuO/CeO_2 catalysts are shown in Fig.S1(see the Electronic Supplementary Material of this paper). There were no Cs species(Cs_2O, CsOH) observed, indicating that the Cs species were well-dispersed on the surface. The average crystal sizes and specific surface areas of the Cs-modified CuO/CeO_2 catalysts are listed in Table 1. It was found that both the crystal size and the surface area of the mixed oxides changed little, indicating that the effect of Cs modification on phase and morphology was slight.

Table 1 Textural properties of the Cs-modified CuO/CeO_2 catalysts

Catalyst	S_{BET}/($m^2·g^{-1}$)	Size of CuO[a]/nm	Size of CeO_2[b]/nm	H_2 uptake of peak α/(mmol·g^{-1})	Area of Cu^+-CO[c]/a.u.	n(Cs)/n(Cu+Ce)[d]	Ce^{3+}(%)	Concentration of surface oxygen[e]/(μmol·g^{-1})	Reaction rate[f]/(μmol·$s^{-1}·g^{-1}$)
CuO/CeO_2	34	27	11	2.00	15.6	—	13.2	277	18.9
0.25%Cs-CuO/CeO_2	36	28	10	3.01	17.8	—	15.7	286	35.6
0.5%Cs-CuO/CeO_2	40	29	10	3.34	19.5	0.004	19.0	364	87.6
1%Cs-CuO/CeO_2	34	31	10	1.10	10.2	0.009	26.5	413	132.9
2%Cs-CuO/CeO_2	28	30	10	0.59	7.7	0.022	23.3	336	51.2
4%Cs-CuO/CeO_2	32	28	11	0.35	5.0	0.048	16.7	289	44.2

a. Calculated from the CuO phase(2θ=35.4°) by Scherrer's equation; *b*. calculated from the CeO_2 phase(2θ=28.5°) by Scherrer's equation; *c*. areas of the IR peak of Cu^+-CO at 2100 cm^{-1}; *d*. calculated from XPS analysis; *e*. calculated from the peak area of O_2-TPD; *f*. calculated at 300 °C.

It has been reported that small amounts of alkali ions can stabilize lower valence states[20,21]. XPS experiments were conducted to obtain information on the valence states of Cu and Ce. Fig.S2(see the Electronic Supplementary Material of this paper) exhibits the Cu_{2p} spectra obtained from catalysts with various Cs contents. The peaks at a binding energy of 934.0 eV, assigned to $Cu_{2p_{3/2}}$, barely changed, indicating that Cu mainly existed in the form of Cu^{2+} and was not influenced by Cs modification[13].

Fig.1 shows the XPS spectra of Ce_{3d}. According to the reported data[24,25], peaks labeled v, v″ and v‴ are attributable to the $Ce_{3d_{5/2}}$ photoelectron emission of Ce^{4+}, while peaks labeled u, u″ and u‴ are due to the $Ce_{3d_{3/2}}$ of Ce^{4+}. Peaks labeled v′, v′$_0$ and u′, u′$_0$(green color-filled curves) are attributable to the $3d_{5/2}$ and $3d_{3/2}$ electrons of Ce^{3+}, respectively. The Ce^{3+} percentages of various Cs-modified CuO/CeO_2 were calculated from the corresponding peak areas(the green area/the whole area) and have been listed in Table 1. The Ce^{3+} percentage significantly increased with the modification of Cs, and 1%Cs-CuO/CeO_2 contained the highest Ce^{3+} percentage, which was almost twice as much as CuO/CeO_2, indicating that the Cs electron donor had a strong interaction with the CeO_2 and effectively

improved the stability of Ce^{3+}[25]. The increase in Ce^{3+} content produced more oxygen vacancies, which could enhance oxygen migration. The further increase in Cs content led to the decrease of Ce^{3+}, probably due to the inhibiting counter effect as reported[21].

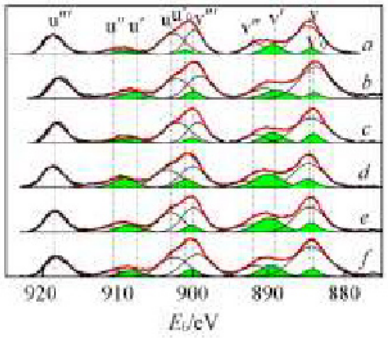

Fig.1 XPS spectra of Ce_{3d} obtained on Cs-modified CuO/CeO_2 catalysts

a. CuO/CeO_2; *b*. 0.25%Cs-CuO/CeO_2; *c*. 0.5%Cs-CuO/CeO_2; *d*. 1%Cs-CuO/CeO_2; *e*. 2%Cs-CuO/CeO_2; *f*. 4%Cs-CuO/CeO_2.

The reducibility change caused by Cs modification was visualized by H_2-TPR(Fig.2). According to previous works[15,16,26], the peaks from 100 °C to 300 °C related to the reduction of various CuO species; peak α corresponded to the reduction of highly dispersed CuO that had a strong synergic effect with CeO_2, and this CuO species was regarded as the main active site[13,15]; peak β corresponded to the reduction of larger CuO clusters or bulk CuO, which had weak or no interactions with CeO_2. The H_2 consumption of peak α is shown in Table 1. We found that the addition of Cs slightly influenced the strong effect between CuO and CeO_2. With the increase in Cs content, the area of peak α increased at first and the reduction temperatures of both peaks did not change until the Cs content reached 0.5%, indicating the improvement of reducibility by Cs modification. However, the area of peak α decreased dramatically, and peak β shifted to a higher temperature upon excessive Cs loading. This indicated a decrease of reducibility because excessive Cs could migrate to the Cu surface, leading to reduction-inhibiting effects[27].

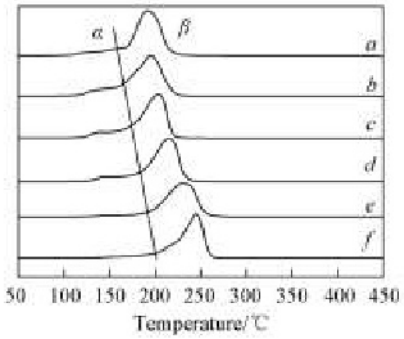

Fig.2 H_2-TPR profiles of Cs-modified CuO/CeO_2 catalysts

a. CuO/CeO_2; *b*. 0.25%Cs-CuO/CeO_2; *c*. 0.5%Cs-CuO/CeO_2; *d*. 1%Cs-CuO/CeO_2; *e*. 2%Cs-CuO/CeO_2; *f*. 4%Cs-CuO/CeO_2.

Previous works[13,15—18] revealed that the catalytic decomposition of N_2O over Cu-Ce mixed oxide catalysts took place on Cu^+ sites. IR was used as a powerful method to detect and measure the number of Cu^+ active sites[13,16]. Fig.3 exhibits the CO-IR spectra of Cs-modified CuO/CeO_2 catalysts at 50 °C after being heated in He at 400 °C for 1 h. The peaks at approximately 2080 cm^{-1} are related to Cu^+-CO[13,16], and the peak areas are listed in Table 1. It was found that the amount of Cu^+ increased at first with the addition of Cs and reached a maximum level at 0.5%Cs-CuO/CeO_2, then decreased with higher Cs content. The amount of Cu^+ was proportional to the H_2 consumption of peak α, suggesting that the active Cu^+ came from the reduction of highly dispersed CuO, which had a strong synergic effect with Ce[16]. However, the peak area increased by only 25% at maximum, meaning the promotion effect on the amount of Cu^+ by Cs modification was fairly limited.

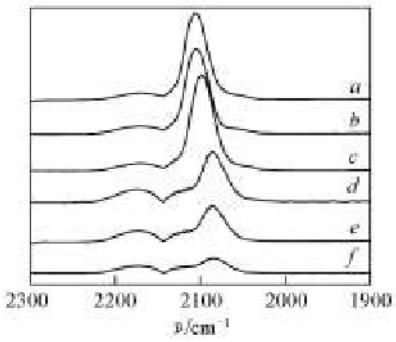

Fig.3 IR spectra recorded of adsorbed CO on Cs-modified CuO/CeO_2 catalysts

a. CuO/CeO_2; *b*. 0.25%Cs-CuO/CeO_2; *c*. 0.5%Cs-CuO/CeO_2; *d*. 1%Cs-CuO/CeO_2; *e*. 2%Cs-CuO/CeO_2; *f*. 4%Cs-CuO/CeO_2.

It is well-known that O_2 desorption is the rate-limiting step in N_2O decomposition, and more Ce^{3+} is generally considered to promote this step[2,3,13—18]. Thus, temperature-programmed desorption(TPD) of O_2 was carried out to investigate the character change of CeO_2 by Cs modification(shown in Fig.4). According to previous works[28,29], the peaks at 100 and 140 °C corresponded to the surface O_2 molecule species, and the peak at approximately 220 °C was assigned to the surface oxygen atom. Both the surface oxygen species were considered to correlate with the activity of N_2O decomposition. Additionally, the lattice oxygen from CeO_2 would desorb at approximately 450 °C. The addition of Cs shifted the surface atom oxygen peak toward lower temperatures and resulted in a massive increase in the peak area(Table 1), indicating that the Cs promoter enhanced the oxygen mobility effectively. The maximum surface-active oxygen was observed with the 1%Cs-CuO/CeO_2

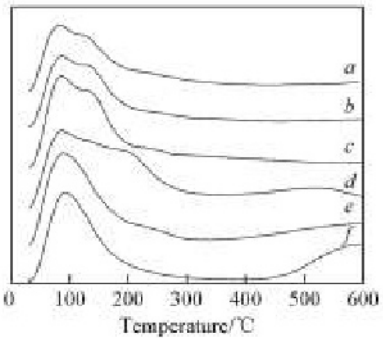

Fig.4 O_2-TPD profiles of Cs-modified CuO/CeO_2 catalysts

a. CuO/CeO_2; *b*. 0.25%Cs-CuO/CeO_2; *c*. 0.5%Cs-CuO/CeO_2; *d*. 1%Cs-CuO/CeO_2; *e*. 2%Cs-CuO/CeO_2; *f*. 4%Cs-CuO/CeO_2.

catalyst.

3.2 Catalytic Performance

The catalytic performances of the catalysts with different Cs contents for N_2O decomposition are shown in Fig.5, and the reaction rates are listed in Table 1. The selectivity for generating N_2 and O_2 was 100%. It was found that the activity for N_2O decomposition was drastically enhanced by Cs modification. It was also found that the activity was related to the content of Ce^{3+}, as the 1%Cs-CuO/CeO_2 with the highest Ce^{3+} percentages showed the best performance, and complete conversion of N_2O was achieved at 380 °C. A further increase in the Cs content resulted in a decrease in the activity, which was also observed over alkali-doped Co_3O_4 catalysts and NiO catalysts[19,20].

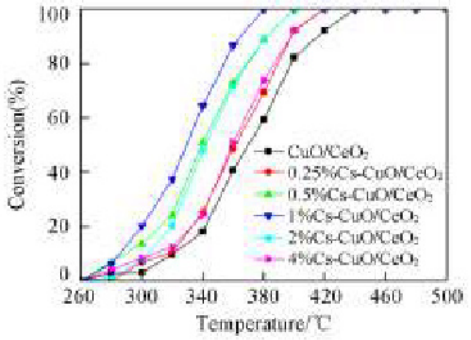

Fig.5 Conversion of N_2O over different Cs-modified CuO/CeO_2 catalysts

Conditions: 2600 μL/L N_2O, balance He, 0.3 MPa, GHSV: 19000 h^{-1}.

To evaluate the effect of Cs modification on oxygen resistance, the conversion of N_2O over CuO/CeO_2 and 1%Cs-CuO/CeO_2 at different reaction conditions is shown in Fig.6. It is obvious that Cs modification exhibited a great promotion effect on oxygen resistance. The conversion of N_2O reached 100% in the presence of O_2 at 380 °C over 1%Cs-CuO/CeO_2, but only reached 5% over CuO/CeO_2 in the same amount of time.

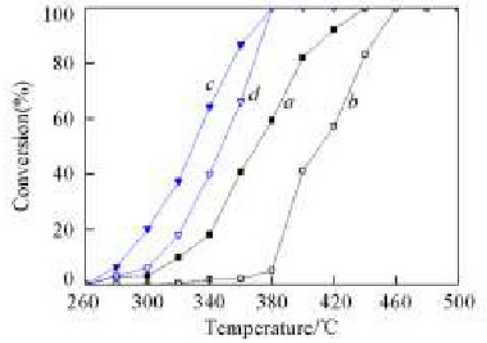

Fig.6 Conversion of N_2O over CuO/CeO_2 and 1%Cs-CuO/CeO_2 under different reaction conditions

a. CuO/CeO_2; *b*. CuO/CeO_2-O_2; *c*. 1%Cs-CuO/CeO_2; *d*. 1%Cs-CuO/CeO_2-O_2. *a*, *c*. 2600 μL/L N_2O+He; *b*, *d*. 2600 μL/L N_2O+2%O_2+He.

3.3 DRIFTs

It is commonly believed that N_2O decomposition over CuO/CeO_2 catalysts mainly proceeds through the following mechanism[13,16]:

$$Cu^{+}+N_2O \rightleftharpoons Cu\text{-}ONN \quad (1)$$

$$Cu\text{-}ONN \longrightarrow Cu^{2+}\text{-}O+N_2 \quad (2)$$

$$2Cu^{2+}\text{-}O \rightleftharpoons 2Cu^{+}+O_2 \quad (3)$$

However, a recent work[17] proposed a new reaction pathway with a different oxygen desorption step:

$$Cu^{2+}\text{-}O+Ce^{3+} \longrightarrow Cu^{+}+Ce^{4+}\text{-}O \quad (4)$$

$$2Ce^{4+}\text{-}O \rightleftharpoons 2Ce^{3+}+O_2 \quad (5)$$

To better understand the relationship between textural properties and catalytic performance, CO-DRIFT was used to investigate the reaction pathway over Cs-modified CuO/CeO_2. Fig.7 exhibits the CO-DRIFTs of the CuO/CeO_2 and 1%Cs-CuO/CeO_2 through different pretreatments. As shown in Fig.7, the peaks at 2120 and 2270 cm^{-1} belonged to the linearly adsorbed Cu^{+} and Ce^{4+} ions, respectively[30—32], while the signal at 2200 cm^{-1} was attributed to gaseous CO. The several peaks in the range from 1200 cm^{-1} to 1700 cm^{-1} belonged to a monodentate carbonate species(1390 and 1480 cm^{-1}) over Ce^{4+} and an asymmetrical inorganic carboxylate species(at approximately 1600 and 1280 cm^{-1}) over Ce^{3+}[30—34]. The shift of the peaks of asymmetrical inorganic carboxylate should be attributed to the electron donation effect of the Cs modification, which caused a weaker C—O bond. These carbon species were considered the products of a CO disproportion reaction taking place on Ce^{3+} ions, which can be confirmed by the appearance of a coke peak at 1250 cm^{-1}[34].

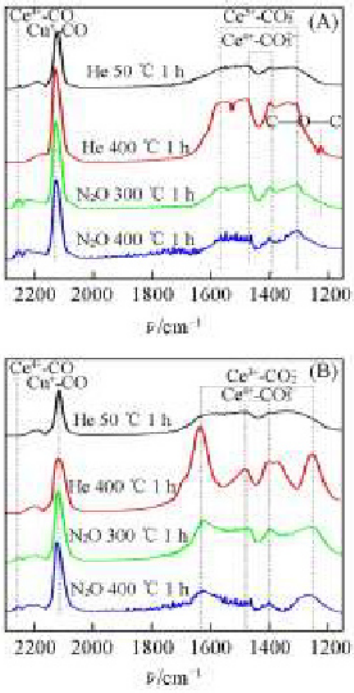

Fig.7 CO-DRIFTs of CuO/CeO_2(A) and 1%Cs-CuO/CeO_2(B) in 1% CO-He at 50 °C for 30 min after different pretreatments

It is obvious that the amounts of Cu^{+} and Ce^{3+} both increased when heated in He, indicating the desorption of active surface oxygen species. After reaction with N_2O, the amount of Ce^{3+} decreased greatly, and the signal of CO-Ce^{4+} appeared over both catalysts, indicating that the Ce^{3+} species were oxidized. We noticed that the CeO_2 did not show any activity at 300 °C, and the Ce-N_2O peak was not detected by *in situ*

N_2O-DRIFTs(Fig.S3, see the Electronic Supplementary Material of this paper)[16,32]. Thus, the oxygen should come from the N_2O decomposition taking place on Cu^+, demonstrating the existence of an oxygen migration step[Eq.(4)].

Peak areas of Cu^+-CO after different pretreatments are shown in Table 2. After a reaction at 300 °C or 400 °C for 1 h, the amount of Cu^+ did not change over that of 1%Cs-CuO/CeO_2, indicating that the oxygen migration, which regenerates Cu^+ from Cu^{2+}-O, can compensate for the loss of Cu^+. On the contrary, the amount of Cu^+ decreased greatly after a reaction in N_2O over unmodified CuO/CeO_2, demonstrating that the oxygen migration step should be the rate limiting step.

Table 2 Peak areas of Cu^+-CO after different pretreatments

Pretreatment	CuO/CeO_2	1%Cs-CuO/CeO_2
He, 50 °C for 1 h	8.2	7.3
He, 400 °C for 1 h	15.6	10.2
1% N_2O, 300 °C for 1 h	14.0	10.4
1% N_2O, 400 °C for 1 h	12.7	10.1

3.4 A Possible Reaction Pathway

Based on previous results, the N_2O decomposition over Cs-modified CuO/CeO_2 proceeded along the following pathway: N_2O was reversibly deposited on the active Cu^+ sites[Eq.(1)], then the activated N—O bond broke, released N_2 and oxidized the Cu^+ to Cu^{2+}-O[Eq.(2)]. Afterwards, Cu^{2+}-O was reduced by Ce^{3+}, Cu^+ was regenerated and formed Ce^{4+}-O[Eq.(4)], and finally, Ce^{4+}—O bonds broke to form O_2[Eq.(5)] as shown in Scheme 1[16]:

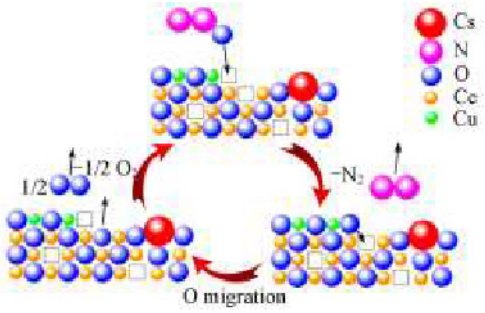

Scheme 1 Possible oxygen migration mechanism over Cs-modified CuO/CeO_2 catalysts

The desorption of generated oxygen was considered as the rate-determining step for N_2O decomposition, so the Ce^{3+} played a key role in the reaction, which was supported by the activity test. Cs modification increased the content of Ce^{3+} dramatically, improved the oxygen mobility and provided more migration sites[Eq.(4)]. Furthermore, it stabilized Ce^{3+} by the electron-donating effect and contributed to the desorption of O_2[Eq.(5)]. Thus, the activity was significantly facilitated. The desorption of generated oxygen is the rate-determining step, and it decides the turnover frequency of Cu^+ sites. Thus, the 1%Cs-CuO/CeO_2 with the best ability of oxygen desorption exhibited the highest activity. Excessive Cs loading resulted in the decrease in Cu^+ and Ce^{3+}, reducing the number and turnover frequency of active sites, finally leading to a reduction in activity.

3.5 Oxygen Inhibition

O_2 is usually present in the N_2O-containing gas stream, and it is known that O_2 will inhibit the activity of N_2O decomposition over a catalyst *via* competitive adsorption with N_2O[14,19]. The 1%Cs-CuO/CeO_2 catalyst exhibited a good performance of oxygen resistance, and it is necessary to explore the reason behind this observation.

Fig.S4(see the Electronic Supplementary Material of this paper) shows the *in situ* N_2O-DRIFTs of 1%Cs-CuO/CeO_2 and CuO/CeO_2 in the presence or absence of O_2. The peak at approximately 2200 cm^{-1} is related to the N_2O absorbed on Cu^+[13,16]. It was found that the competitive adsorption between O_2 and N_2O existed over both catalysts, and it was barely affected by Cs modification, indicating that competitive adsorption was not the main reason for oxygen inhibition. As discussed above, we proposed that the oxygen migration step is the rate-determining step, and O_2 may affect the reaction by inhibiting this step.

CO-DRIFTs through different reactions are shown in Fig.8. It is obvious that the amount of active Cu^+ sites decreased greatly after the reaction with the presence of oxygen over CuO/CeO_2, indicating that oxygen migration was certainly inhibited by O_2. In contrast, the very slight change of Cu^+ over 1%Cs-CuO/CeO_2 indicated an excellent oxygen migration ability, accounting for its great oxygen resistance.

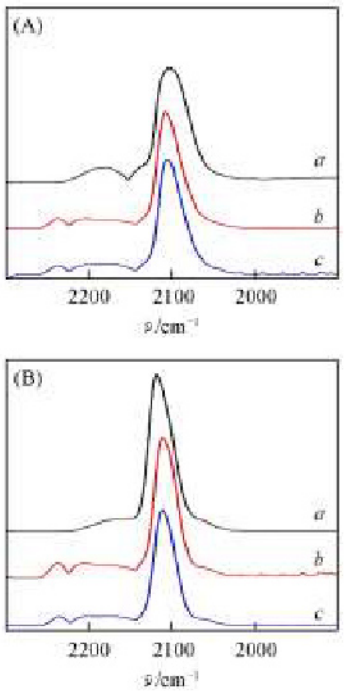

Fig.8 CO-DRIFTs of 1%Cs-CuO/CeO_2(A) and CuO/CeO_2(B) through different reactions

a. He; *b*. 2600 μL/L N_2O+He; *c*. 2600 μL/L N_2O+2%O_2+He.

4 Conclusions

In summary, Cs modification improved stable activity significantly over the CuO/CeO_2 catalysts, and the 1%Cs-CuO/CeO_2 catalyst exhibited the best catalytic performance. CO-DRIFTs revealed that Ce^{3+} could efficiently

facilitate the regeneration of active Cu^{+} sites by an oxygen migration mechanism. Cs modification resulted in an increase in Ce^{3+} content and a promotion of oxygen desorption, which facilitated the regeneration rate of active Cu^{+} sites, thus improving the catalytic activity and oxygen resistance over CuO/CeO_2 catalysts for N_2O decomposition.

Electronic Supplementary Material

Supplementary material is available in the online version of this article at http://dx.doi.org/10.1007/s40242-019-8295-2.

References

[1] Thiemens M. H., Trogler W. C., *Science*, **1991**, *251*, 932

[2] Kapteijn F., Rodriguez-Mirasol J., Moulijn J. A., *Clin. Infect. Dis.*, **2011**, *52*, 1468

[3] Santiago M., Hevia M. A. G., Pérez-Ramírez J., *Appl. Catal. B*, **2009**, *90*, 83

[4] Komvokis V. G., Marti M., Delimitis A., Vasalos I. A., Triantafyllidis K. S., *Appl. Catal. B*, **2011**, *103*, 62

[5] Piumetti M., Hussain M., Fino D., Russo N., *Appl. Catal. B*, **2015**, *165*, 158

[6] Wilczkowska E., Krawczyk K., Petryk J., Sobczak J. W., Kaszkur Z., *Appl. Catal. A*, **2010**, *389*, 165

[7] Christoforou S. C., Efthimiadis E. A., Vasalos I. A., *Catal. Lett.*, **2002**, *79*, 137

[8] Kannan S., Swamy C. S., *Catal. Today*, **1999**, *53*, 725

[9] Pérez-Ramírez J., *J. Catal*., **2004**, *227*, 512

[10] Moretti G., Fierro G., Ferraris G., Andreozzi G. B., Naticchioni V., *J. Catal*., **2014**, *318*, 1

[11] Xie P., Luo Y., Ma Z., Wang L., Huang C., Yue Y., Hua W., Gao Z., *Appl. Catal. B*, **2015**, *170*, 34

[12] Perez-Alonso F. J., Melián-Cabrera I., Granados M. L., Kapteijn F., Fierro J. L. G., *J. Catal*., **2006**, *239*, 340

[13] Zhou H., Huang Z., Sun C., Qin F., Xiong D., Shen W., Xu H., *Appl. Catal. B*, **2012**, *125*, 492

[14] Zhou H., Hu P., Zhen H., Feng Q., Wei S., Xu H., *Ind. Eng. Chem. Res.*, **2013**, *52*, 4504

[15] Zabilskiy M., Erjavec B., Djinović P., Pintar A., *Chem. Eng. J.*, **2014**, *254*, 153

[16] Zabilskiy M., Djinović P., Tchernychova E., Tkachenko O. P., Kustov L. M., Pintar A., *ACS Catal.*, **2015**, *5*, 5357

[17] Zabilskiy M., Djinović P., Tchernychova E., Pintar A., *Appl. Catal. B*, **2016**, *197*, 146

[18] Konsolakis M., Carabineiro S. A. C., Papista E., Tavares P. B., Agostinho Moreira J., Romaguera-Barcelayf Y., Figueiredob J. L., *Catal. Sci. Tech.*, **2015**, *5*, 3714

[19] Ohnishi C., Asano K., Iwamoto S., Chikama K., Inoue M., *Catal. Today*, **2007**, *120*, 145

[20] Pasha N., Lingaiah N., Siva Sankar Reddy P., Sai Prasad P. S., *Catal. Lett.*, **2007**, *118*, 64

[21] Pasha N., Lingaiah N., Reddy P. S. S., Prasad P. S. S., *Catal. Lett.*, **2008**, *127*, 101

[22] Grzybek G., Stelmachowski P., Gudyka S., Duch J., Ćmil K., Kotarba A., *Appl. Catal. B*, **2015**, *168*, 509

[23] Xue L., He H., Liu C., Zhang C., Zhang B., *Environ. Sci. Technol*., **2009**, *43*, 890

[24] Yu Q. Q., Li Y., Zou X. H., Zhuo H. Y., Yao Y. Y., Suo Z. H., *Chinese J. Catal.*, **2010**, *31*, 671

[25] Torsten B., Christian E., Ken-ichi I., Bernd S., *Chem. Mater.*, **2005**, *17*, 1683

[26] Caputo T., Lisi L., Pirone R., Russo G., *Appl. Catal. A*, **2008**, *348*, 42

[27] Aika K. I., Hori H., Ozaki A., *J. Catal.*, **1972**, *27*, 424

[28] Ma C., Wang D., Xue W., Dou B., Wang H., Hao Z., *Environ Sci. Technol.*, **2011**, *45*, 3628

[29] Ma L., Wang D., Li J., Bai B., Fu L., Li Y., *Appl. Catal. B*, **2014**, *148/149*, 36

[30] Liu L., Liu B., Dong L., Zhu J., Wan H., Sun K., Zhao B., Zhu H., Dong L., Chen Y., *Appl. Catal. B*, **2009**, *90*, 578

[31] Liu Y., Wen, C., Yun G., Liu X., Ren J., Lu G., Wang Y., *Chem. Cat. Chem.*, **2010**, *2*, 336

[32] Polster C. S., Nair H., Baertsch C. D., *J. Catal*., **2009**, *266*, 308

[33] Martínez-Arias A., Hungría A. B., Fernández-García M., Conesa J. C., Munuera G., *J. Power Sources*, **2005**, *151*, 32

[34] Marbán G., López I., Valdés-Solís T., *Appl. Catal. B*, **2009**, *361*, 160